Applied Physics Letters

Anomalous Hall effect in thin films of the Weyl antiferromagnet Mn_3Sn

Cite as: Appl. Phys. Lett. **113**, 202402 (2018); https://doi.org/10.1063/1.5064697
Submitted: 07 October 2018 . Accepted: 26 October 2018 . Published Online: 15 November 2018

Tomoya Higo, Danru Qu, Yufan Li, C. L. Chien, Yoshichika Otani, and Satoru Nakatsuji

COLLECTIONS

This paper was selected as Featured

View Online Export Citation CrossMark

ARTICLES YOU MAY BE INTERESTED IN

Anomalous Hall effect in polycrystalline Mn_3Sn thin films
Applied Physics Letters **113**, 222405 (2018); https://doi.org/10.1063/1.5051495

Magnetic phase dependence of the anomalous Hall effect in Mn_3Sn single crystals
Applied Physics Letters **112**, 132406 (2018); https://doi.org/10.1063/1.5021133

Angle dependent magnetoresistance in heterostructures with antiferromagnetic and non-magnetic metals
Applied Physics Letters **113**, 202404 (2018); https://doi.org/10.1063/1.5049566

Challenge us.
What are your needs for periodic signal detection?
Zurich Instruments
Watch

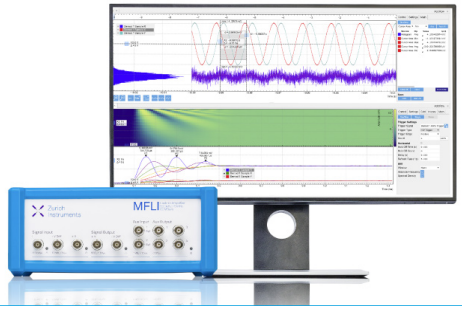

© 2018 Author(s).

Anomalous Hall effect in thin films of the Weyl antiferromagnet Mn_3Sn

Tomoya Higo,[1,2] Danru Qu,[1] Yufan Li,[3] C. L. Chien,[3] Yoshichika Otani,[1,2,4] and Satoru Nakatsuji[1,2,5,a)]
[1]*Institute for Solid State Physics, University of Tokyo, Kashiwa, Chiba 277-8581, Japan*
[2]*CREST, Japan Science and Technology Agency (JST), Kawaguchi, Saitama 332-0012, Japan*
[3]*Department of Physics and Astronomy, Johns Hopkins University, Baltimore, Maryland 21218, USA*
[4]*Center for Emergent Matter Science, RIKEN, Wako, Saitama 351-0198, Japan*
[5]*Institute for Quantum Matter and Department of Physics and Astronomy, Johns Hopkins University, Baltimore, Maryland 21218, USA*

(Received 7 October 2018; accepted 26 October 2018; published online 15 November 2018)

The Weyl antiferromagnet Mn_3Sn has been recently attracting significant attention as it exhibits various useful functions such as a large anomalous Hall effect that is normally absent in antiferromagnets. Here, we report the thin film fabrication of the single phase of Mn_3Sn and the observation of the large anomalous Hall effect at room temperature despite its vanishingly small magnetization. Our work on the high-quality thin film growth of the Weyl antiferromagnet paves the path for developing antiferromagnetic spintronics. *Published by AIP Publishing.*
https://doi.org/10.1063/1.5064697

Recent rapid growth in information technology has demanded the spintronic devices to acquire higher integration density and faster data processing, for instance, in nonvolatile magnetic memory devices.[1] For these requirements, antiferromagnets have been attracting much attention recently as an important material for next generation memory devices, because they generate no perturbing stray field and have much faster spin dynamics than ferromagnets.[2–14] On the other hand, it is also true that the absence of magnetization, which is the reason for the above benefits, have made it notoriously difficult to control and otherwise produce only very weak responses to detect them.

In this context, the recent discovery of functional antiferromagnets $D0_{19}$ Mn_3X (X = Sn, Ge), the first example of a topological "Weyl magnet," has attracted a lot of attention.[8–10,15–19] This is because it exhibits a variety of useful functions that have never been seen in antiferromagnets at zero magnetic field, which include (1) the anomalous Hall effect,[8–10] (2) the anomalous Nernst effect,[15,16] and (3) the magneto-optical Kerr effect[18] at room temperature. Moreover, they are controllable by a magnetic field and thus can be used for designing antiferromagnetic spintronics and in energy harvesting technology. It has been shown that the antiferromagnet exhibiting these effects hosts the topological state called the magnetic Weyl metal, characterized by relativistic Weyl fermions.[17,19] The discovery of the Weyl metal state in an antiferromagnet represents the opening of another chapter of applied research using the functional antiferromagnets and it is thus highly important to fabricate a high-quality thin film of the Weyl antiferromagnet.

$D0_{19}$ Mn_3Sn has a hexagonal Ni_3Sn-type structure with space group $P6_3/mmc$ [Fig. 1(a)]. The basal plane projection of each (0001) plane consists of a kagome lattice of Mn magnetic atoms, and the associated geometrical frustration manifests itself as an inverse triangular spin structure, which is of antiferromagnetic ordering with very small net magnetic moments of ∼3 mμ_B/Mn, below the Néel point T_N ∼ 420 K.[20,21] As shown in Fig. 1(b), this unique antiferromagnetic spin structure within the (0001) plane can be characterized by a ferroic ordering of a cluster-octupole moment consisting of non-collinear spins on the Kagome bilayer.[22] Thus, unlike a normal antiferromagnetic state, this breaks time-reversal symmetry (TRS) macroscopically. In ferromagnets, it is the spontaneous magnetization that breaks TRS, and the anomalous Hall effect appears proportionally to the magnetization based on the mechanisms including side jump scattering, skew scattering, and intrinsic (Berry curvature) effects.[23] In Weyl magnets, on the other hand, the anomalous Hall effect arises from an intrinsic mechanism that is associated with the large Berry curvature due to the Weyl fermions, and thus it is not necessary to be proportional to the magnetization.[8–10,15–19] In Mn_3Sn, the TRS breaking by the noncollinear antiferromagnetic order leads to the formation of Weyl points[15–19] and the sizable Berry curvature or fictitious field corresponding to the external magnetic field of ∼100 T in the momentum space even with a vanishingly small FM moment of ∼3 mμ_B/Mn.[17,19,22] As a result, this magnetic Weyl metal state exhibits large topological responses (e.g., the anomalous Hall effect), comparable to those in ferromagnets.

Here, we report the fabrication of a high-quality thin film of Mn_3Sn that exhibits the anomalous Hall effect at room temperature. We find that a single phase polycrystalline thin film of Mn_3Sn can be deposited onto a Si/SiO_2 substrate. Our measurements of the Hall effect indicate that the film shows approximately half the size of the anomalous Hall effect compared to the values reported for single crystals.[8,15–18] Our work on the high-quality thin film growth paves the path for developing antiferromagnetic spintronics and energy harvesting technology by using Weyl magnets.

For the thin film fabrication, we employ DC magnetron sputtering. The films are deposited at room temperature onto a Si/SiO_2 substrate from the $Mn_{2.5}Sn$ target in a chamber with a base pressure of 5×10^{-7} Pa. The sputtering power and the Ar gas pressure are 60 W and 0.3 Pa, respectively.

a)E-mail: satoru@issp.u-tokyo.ac.jp

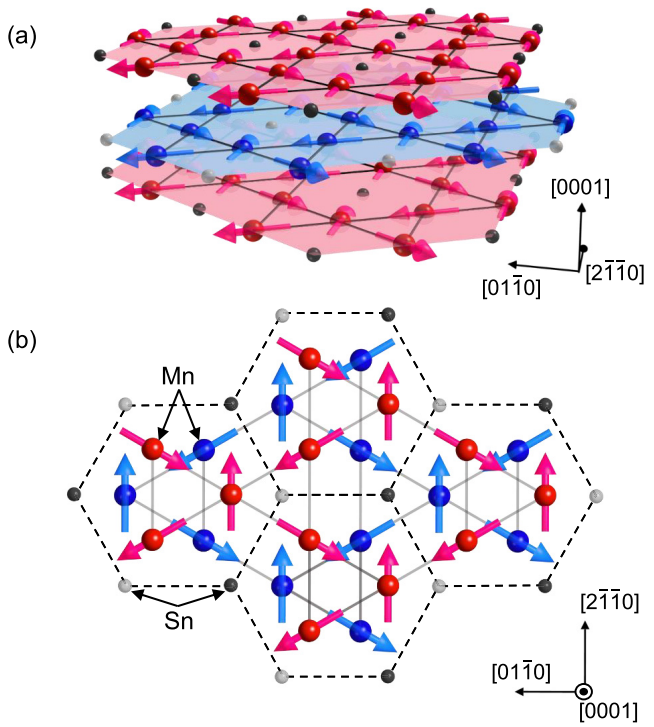

FIG. 1. 3D view (a) and top view along the (0001) direction (b) of the crystal and magnetic structures of the Weyl antiferromagnet Mn_3Sn. The large red and blue spheres (small black and gray spheres) represent Mn atoms (Sn atoms) at $z = 0$ and 1/2, respectively. The Mn magnetic moments (arrows) lie in the (0001)-plane and form an inverse triangular spin structure. The spin structure on the kagome bilayers can be considered as ferroic ordering of a cluster magnetic octupole. The octupole unit is represented by a hexagon in Fig. 1(b).

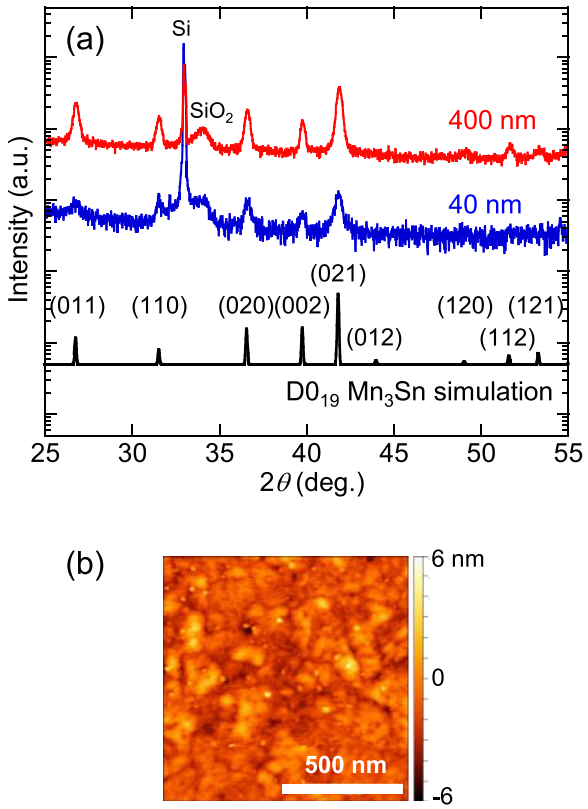

FIG. 2. (a) Room temperature spectra obtained with an X-ray diffractometer (CuKα1 with a wavelength of 1.54059 Å) for the 40 and 400 nm thin films of Mn_3Sn on a Si/SiO_2 substrate. The theoretical spectrum of the $D0_{19}$ Mn_3Sn structure is presented at the bottom. (b) Surface topography of the Mn_3Sn (40 nm) thin film obtained by atomic force microscopy (AFM). The scan area is 1 μm × 1 μm.

For this condition, our X-ray reflectivity measurements find the deposition rate to be ~0.2 nm/s. During the deposition, we rotate the sample holder along its normal axis to ensure a uniform composition and thickness. After deposition at room temperature, we anneal the film at 500 °C for 1 h. The annealing procedure after the deposition crystallizes the as-deposited amorphous film in a polycrystalline form of the Mn_3Sn film. The composition of the film is estimated to be $Mn_{3.05}Sn_{0.95}$ by inductively coupled plasma atomic emission spectroscopy (ICP-AES). We note that the Mn composition of our film is within the range of the composition, $Mn_{3.02}Sn_{0.98}$-$Mn_{3.15}Sn_{0.85}$, where the $D0_{19}$ Mn_3Sn phase is reported to be stable due to the presence of excess Mn, which randomly occupies the Sn site.[8,20,21] Structural analysis is performed by X-ray diffraction (XRD) spectroscopy. The magnetization is measured with a commercial SQUID magnetometer (MPMS, Quantum Design). To estimate the signal from the samples, the diamagnetic contribution of the Si/SiO_2 substrate is separately measured and subtracted from the magnetization. Both longitudinal and Hall resistivity (ρ_{xx} and ρ_{yx}) are measured by a standard four-probe method using a variable temperature insert (VTI) with a superconducting magnet (Teslatron PT, Oxford Instruments) and a commercial physical property measurement system (PPMS, Quantum Design). The samples are patterned into standard Hall bars for electrical transport measurements. The Hall resistivity ρ_{yx} is defined as $V_y \cdot d/I_x$, where I_x, V_y, and d stand for the current, the transverse voltage and the thickness, respectively. The field dependence of the Hall resistivity is obtained after subtracting the longitudinal resistivity contribution, which presumably originates from slight misalignment of the Hall probes and is even-symmetric to the applied field.

The crystallinity of the film is examined by the XRD method. Figure 2(a) shows the XRD patterns of the post-annealed Mn_3Sn (40 and 400 nm) films. Significantly, we confirm the films to be of the single phase of Mn_3Sn and in a randomly oriented polycrystalline form; all the peaks can be indexed by the Bravais lattice with the lattice constants $a = 5.67$ Å and $c = 4.52$ Å consistent with the hexagonal $P6_3/mmc$ symmetry of $D0_{19}$ Mn_3Sn, and there are no additional peaks coming from plausible impurity phases such as ferromagnetic Mn_2Sn and Mn_3Sn_2. The ratio of the peak intensity is found to be roughly consistent with the theoretical simulation [the bottom curve in Fig. 2(a)], except for the ratio between (011) and (002) for the 400 nm film. This suggests that the 400 nm film has a slightly larger population of the grain having the (011) plane parallel to the film surface than the ideal polycrystalline distribution. The surface morphology is examined by atomic force microscopy (AFM) method. As can be seen in Fig. 2(b), the AFM scan image over 1 μm × 1 μm area of the post-annealed film (40 nm) reveals a relatively rough surface with a typical root mean square surface roughness of ~1.1 nm because of the multi-grain character.

To clarify the magnetic phase of the Mn_3Sn films and verify the absence of ferromagnetic impurity as found in the

XRD measurements, we perform the magnetization measurements. Figure 3(a) shows the temperature (T) dependence of the zero-field out-of-plane magnetization $M(H=0)$ of the Mn_3Sn film obtained from 300 K to 100 K on cooling after the demagnetization process (we first applied a field of $\mu_0 H = 5$ T perpendicular to the film surface and decreased the field down to 0 T at 300 K). The zero-field magnetization exhibits an abrupt decrease below $T_1 = 260$ K, corresponding to the magnetic phase transition known for Mn_3Sn, namely from the inverse triangular spin structure to the helical (spiral) spin structure on cooling.[24,25] This result provides strong evidence that the magnetic state is the same as the bulk Mn_3Sn and large topological responses such as the anomalous Hall effect is expected in the high temperature phase with an inverse triangular spin structure. The spontaneous magnetization value at 100 K is as low as $\sim$0.1 mμ_B/Mn close to the resolution of our measurements. This further confirms the absence of ferromagnetic impurity in our film. Figure 3(b) shows the field dependence of the magnetization obtained under a field of up to 5 T at room temperature. The magnetization M exhibits a hysteresis with the spontaneous component of 6 mμ_B/Mn (2.6 kA/m) at $H=0$. In the case of single crystals of Mn_3Sn, the spontaneous M is anisotropic; it is $\sim$3 mμ_B/Mn for the field along the (0001) plane (ab-plane), while it is absent in the [0001] direction (c-axis).[8] Thus, the polycrystalline average is $\sim$2 mμ_B/Mn, which is on the order of our polycrystalline film.

Most significantly, for the Weyl antiferromagnet Mn_3Sn, the sizeable anomalous Hall effect emerges in the magnetic Weyl metal state with the inverse triangular spin structure. Figure 4(a) provides the T dependence of the longitudinal resistivity ρ_{xx} and the spontaneous Hall resistivity $\rho_{yx}(H=0)$ under zero field of the Mn_3Sn thin film (40 nm). The resistivity $\rho_{xx}(T)$ confirms the metallic transport

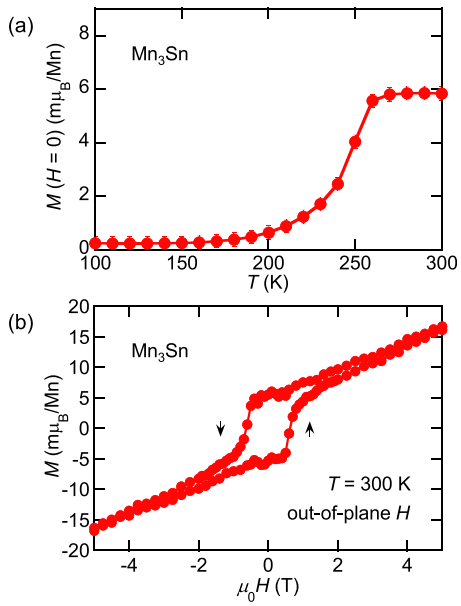

FIG. 3. (a) Temperature dependence of the zero-field perpendicular magnetization of the Mn_3Sn (400 nm) thin film. (b) Field dependence of the magnetization measured under the magnetic field applied in the perpendicular direction to the surface of the Mn_3Sn (400 nm) thin film. The arrows indicate the direction of the field sweep.

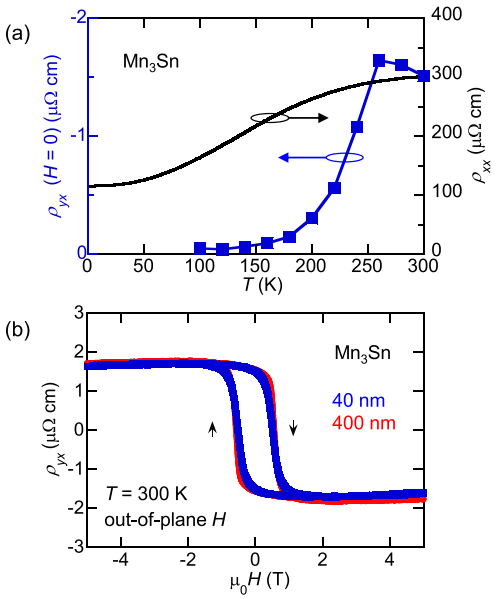

FIG. 4. (a) Temperature dependence of the resistivity and the spontaneous Hall resistivity of the Mn_3Sn (40 nm) thin film. (b) Field dependence of the Hall resistivity ρ_{yx} measured under the magnetic field applied in the perpendicular direction to the surface of the Mn_3Sn (40 and 400 nm) thin films. The sign of Hall resistivity ρ_{yx} is negative under a positive field larger than the coercivity. The arrows indicate the direction of the field sweep.

consistent with the previous work on bulk single crystals.[8,15–18] The zero-field Hall resistivity $\rho_{yx}(H=0)$ was obtained from $(\rho_{yx}(H=+0) - \rho_{yx}(H=-0))/2$. Here, we use $+0$ and -0 to indicate zero magnetic field approached, respectively, from $+5$ T and -5 T in the measurement of the spontaneous component of the Hall resistivity at each temperature. Similar to the magnetization, we observe a sharp decrease in $\rho_{yx}(H=0)$ below $T_1 = 260$ K on cooling; this agrees with the magnetic symmetry consideration in Mn_3Sn that the inverse triangular spin structure breaks the global time-reversal symmetry, while it is restored in the low temperature helical phase. Figure 4(b) indicates the field dependence of the Hall resistivity ρ_{yx} at 300 K as a function of the magnetic field applied perpendicular to the film surface. The anomalous Hall effect of the 40 nm film exhibits a large change in ρ_{yx} from 1.5 $\mu\Omega$ cm to -1.5 $\mu\Omega$ cm with increasing field because of the switching of the antiferromagnetic domain in the real space and the large fictitious field in the momentum space, and nearly the same field dependence is observed for the 400 nm film. The coercivity is found to be 0.6 T, consistent with the results seen in the magnetization curve [Fig. 3(b)]. All the ferromagnetic impurities known for the Mn-Sn binary system have the Curie temperature lower than the room temperature. Thus, the large spontaneous Hall effect with vanishingly small magnetization seen at 300 K and the T dependence of the Hall effect and the magnetization having clear suppression below T_1 provide good evidence that the film is of single phase and it is the inverse triangular spin state of the Mn_3Sn polycrystalline phase at $T > T_1$ that exhibits the large anomalous Hall effect.

Here, we note that no report has been made on the thin film of the antiferromagnetic Mn_3X film exhibiting the large anomalous Hall effect, having the same order of magnitude as the value reported for bulk. In fact, the literature on the

epitaxial thin film fabrication of Mn_3Sn has been published,[26] but without showing any results on anomalous Hall effect. They find that their film has one order larger magnetization than what has been seen in single crystals, suggesting the defect and/or inclusion of ferromagnetic impurity. The comparison with our results indicates that the fabrication of the single phase and appropriate Mn concentration are the keys for the observation of the anomalous Hall effect.

Our fabrication of the high-quality thin film of the Weyl antiferromagnet Mn_3Sn and observation of its large anomalous Hall effect provide an important step for further developing devices useful for antiferromagnetic spintronics such as for high-speed and high-density information storage.

We thank T. Nishikawa, T. Ohtsuki, H. Man, Q. Ma, A. Kobayashi, K. Kondou, P. K. Muduli, and S. Miwa for helpful discussions. We also thank R. Ishii for the ICP-AES measurements, and M. Lippmaa, J. Lee, and R. Takahashi for the AFM measurements and device fabrication. This work was partially supported by CREST (Nos. JPMJCR15Q5 and JPMJCR18T3), Japan Science and Technology Agency, by Grants-in-Aid for Scientific Research (No. 16H02209), and by Grants-in-Aid for Scientific Research on Innovative Areas (Nos. 15H05882, 15H05883, and 26103002) from the Ministry of Education, Culture, Sports, Science, and Technology of Japan, and Program for Advancing Strategic International Networks to Accelerate the Circulation of Talented Researchers (No. R2604) from the JSPS. D.Q. was supported by the JSPS as an international research fellow. The work at JHU was supported in part by SHINES Grant No. DE-SC0012670, an Energy Frontier Research Center from the U.S. Department of Energy, Office of Science, Basic Energy Science. The work at IQM was supported as part of the Institute for Quantum Matter, an Energy Frontier Research Center funded by the U.S. Department of Energy, Office of Science, Office of Basic Energy Sciences under Award No. DE-SC0019331.

[1]C. Chappert, A. Fert, and F. N. Van Dau, Nat. Mater. **6**, 813 (2007).
[2]A. S. Núñez, R. A. Duine, P. Haney, and A. H. MacDonald, Phys. Rev. B **73**, 214426 (2006).
[3]A. B. Shick, S. Khmelevskyi, O. N. Mryasov, J. Wunderlich, and T. Jungwirth, Phys. Rev. B **81**, 212409 (2010).
[4]A. H. MacDonald and M. Tsoi, Philos. Trans. R. Soc. A **369**, 3098 (2011).
[5]B. G. Park, J. Wunderlich, X. Marti, V. Holy, Y. Kurosaki, M. Yamada, H. Yamamoto, A. Nishide, J. Hayakawa, H. Takahashi, A. B. Shick, and T. Jungwirth, Nat. Mater. **10**, 347 (2011).
[6]X. Marti, I. Fina, C. Frontera, J. Liu, P. Wadley, Q. He, R. J. Paull, J. D. Clarkson, J. Kudrnovský, I. Turek, J. Kuneš, D. Yi, J.-H. Chu, C. T. Nelson, L. You, E. Arenholz, S. Salahuddin, J. Fontcuberta, T. Jungwirth, and R. Ramesh, Nat. Mater. **13**, 367 (2014).
[7]E. V. Gomonay and V. M. Loktev, Low Temp. Phys. **40**, 17 (2014).
[8]S. Nakatsuji, N. Kiyohara, and T. Higo, Nature **527**, 212 (2015).
[9]N. Kiyohara, T. Tomita, and S. Nakatsuji, Phys. Rev. Appl. **5**, 064009 (2016).
[10]A. K. Nayak, J. E. Fischer, Y. Sun, B. Yan, J. Karel, A. C. Komarek, C. Shekhar, N. Kumar, W. Schnelle, J. Kübler, C. Felser, and S. S. P. Parkin, Sci. Adv. **2**, e1501870 (2016).
[11]P. Wadley, B. Howells, J. Železný, C. Andrews, V. Hills, R. P. Campion, V. Novák, K. Olejník, F. Maccherozzi, S. S. Dhesi, S. Y. Martin, T. Wagner, J. Wunderlich, F. Freimuth, Y. Mokrousov, J. Kuneš, J. S. Chauhan, M. J. Grzybowski, A. W. Rushforth, K. W. Edmonds, B. L. Gallagher, and T. Jungwirth, Science **351**, 587 (2016).
[12]T. Jungwirth, X. Marti, P. Wadley, and J. Wunderlich, Nat. Nanotechnol. **11**, 231 (2016).
[13]L. Šmejkal, Y. Mokrousov, B. Yan, and A. H. MacDonald, Nat. Phys. **14**, 242–251 (2018).
[14]V. Baltz, A. Manchon, M. Tsoi, T. Moriyama, T. Ono, and Y. Tserkovnyak, Rev. Mod. Phys. **90**, 015005 (2018).
[15]M. Ikhlas, T. Tomita, T. Koretsune, M.-T. Suzuki, D. Nishio-Hamane, R. Arita, Y. Otani, and S. Nakatsuji, Nat. Phys. **13**, 1085 (2017).
[16]X. Li, L. Xu, L. Ding, J. Wang, M. Shen, X. Lu, Z. Zhu, and K. Behnia, Phys. Rev. Lett. **119**, 056601 (2017).
[17]K. Kuroda, T. Tomita, M.-T. Suzuki, C. Bareille, A. A. Nugroho, P. Goswami, M. Ochi, M. Ikhlas, M. Nakayama, S. Akebi, R. Noguchi, R. Ishii, N. Inami, K. Ono, H. Kumigashira, A. Varykhalov, T. Muro, T. Koretsune, R. Arita, S. Shin, T. Kondo, and S. Nakatsuji, Nat. Mater. **16**, 1090 (2017).
[18]T. Higo, H. Man, D. B. Gopman, L. Wu, T. Koretsune, O. M. J. van 't Erve, Y. P. Kabanov, D. Rees, Y. Li, M.-T. Suzuki, S. Patankar, M. Ikhlas, C. L. Chien, R. Arita, R. D. Shull, J. Orenstein, and S. Nakatsuji, Nat. Photonics **12**, 73 (2018).
[19]H. Yang, Y. Sun, Y. Zhang, W.-J. Shi, S. S. P. Parkin, and B. Yan, New J. Phys. **19**, 015008 (2017).
[20]S. Tomiyoshi and Y. Yamiguchi, J. Phys. Soc. Jpn. **51**, 2478 (1982).
[21]P. J. Brown, V. Nunez, F. Tasset, J. B. Forsyth, and P. Radhakrishna, J. Phys. Condens. Matter. **2**, 9409 (1990).
[22]M.-T. Suzuki, T. Koretsune, M. Ochi, and R. Arita, Phys. Rev. B **95**, 094406 (2017).
[23]N. Nagaosa, J. Sinova, S. Onoda, A. H. MacDonald, and N. P. Ong, Rev. Mod. Phys. **82**, 1539 (2010).
[24]T. F. Duan, W. J. Ren, W. L. Liu, S. J. Li, W. Liu, and Z. D. Zhang, Appl. Phys. Lett. **107**, 082403 (2015).
[25]N. H. Sung, F. Ronning, J. D. Thompson, and E. D. Bauer, Appl. Phys. Lett. **112**, 132406 (2018).
[26]A. Markou, J. M. Taylor, A. Kalache, P. Werner, S. S. P. Parkin, and C. Felser, Phys. Rev. Mater. **2**, 051001 (2018).